Bortezomib-Resistant Nuclear Factor-κB Activity in Multiple Myeloma Cells

Stephanie Markovina,[1,2] Natalie S. Callander,[3,4] Shelby L. O'Connor,[2] Jihoon Kim,[5] Jae E. Werndli,[3] Martha Raschko,[3] Catherine P. Leith,[4,6] Brad S. Kahl,[3,4] KyungMann Kim,[4,5] and Shigeki Miyamoto[1,2,4]

[1]Program in Cellular and Molecular Biology and Medical Scientist Training Program, [2]Department of Pharmacology, [3]Division of Hematology, Department of Medicine, [4]University of Wisconsin Comprehensive Cancer Center, [5]Program in Statistics, Department of Statistics, and [6]Division of Hematopathology, Department of Pathology, University of Wisconsin School of Medicine and Public Health, Madison, Wisconsin

Abstract

Bortezomib (Velcade/PS341), a proteasome inhibitor used in the treatment of multiple myeloma (MM), can inhibit activation of nuclear factor-κB (NF-κB), a family of transcription factors often deregulated and constitutively activated in primary MM cells. NF-κB can be activated via several distinct mechanisms, including the proteasome inhibitor–resistant (PIR) pathway. It remains unknown what fraction of primary MM cells harbor constitutive NF-κB activity maintained by proteasome-dependent mechanisms. Here, we report an unexpected finding that constitutive NF-κB activity in 10 of 14 primary MM samples analyzed is refractory to inhibition by bortezomib. Moreover, when MM cells were cocultured with MM patient-derived bone marrow stromal cells (BMSC), microenvironment components critical for MM growth and survival, further increases in NF-κB activity were observed that were also refractory to bortezomib. Similarly, MM-BMSCs caused PIR NF-κB activation in the RPMI8226 MM cell line, leading to increased NF-κB–dependent transcription and resistance to bortezomib-induced apoptosis.

Our findings show that primary MM cells frequently harbor PIR NF-κB activity that is further enhanced by the presence of patient-derived BMSCs. They also suggest that this activity is likely relevant to the drug resistance development in some patients. Further elucidation of the mechanism of PIR NF-κB regulation could lead to the identification of novel diagnostic biomarkers and/or therapeutic targets for MM treatment. (Mol Cancer Res 2008;6(8):1356–64)

Received 2/23/08; revised 4/24/08; accepted 5/5/08.

Grant support: Predoctoral NIH Fellowship in Hematology Research T32 HL07899, Predoctoral National Institute of Aging Fellowship F30-AG029714-01 (S. Markovina), NIH grant R01-CA08106, University of Wisconsin Trillium Foundation Grant, and Shaw Scientist Award from Milwaukee Foundation (S. Miyamoto).

The costs of publication of this article were defrayed in part by the payment of page charges. This article must therefore be hereby marked *advertisement* in accordance with 18 U.S.C. Section 1734 solely to indicate this fact.

Note: Supplementary data for this article are available at Molecular Cancer Research Online (http://mcr.aacrjournals.org/).

Requests for reprints: Shigeki Miyamoto, Department of Pharmacology, University of Wisconsin, 301 SMI, 1300 University Avenue, Madison, WI 53706. Phone: 608-262-9281; Fax: 608-262-1257. E-mail: smiyamot@wisc.edu

doi:10.1158/1541-7786.MCR-08-0108

Introduction

The nuclear factor-κB (NF-κB)/Rel family of transcription factors is composed of five members, p65 (RelA), RelB, cRel, p100/p52, and p105/p50, which bind one another to form homodimers or heterodimers. NF-κB dimers are normally held inactive in the cytoplasm due to association with inhibitor proteins, IκBs. NF-κB can be activated by a wide array of extracellular signals leading to its release from IκBs and translocation to the nucleus where it binds to its cognate κB elements and regulates transcription of genes involved in embryogenesis, innate and adaptive immunity, regulation of cell death, and other physiologic processes (1).

There are two most widely studied mechanisms of NF-κB activation, so-called "canonical" and "noncanonical," which involve signaling events leading to the degradation or processing of inhibitor proteins by the ubiquitin-dependent 26S proteasome system. Thus, these pathways are highly sensitive to inhibition by proteasome inhibitors, including bortezomib (Velcade/PS341), the first proteasome inhibitor approved for clinical use (2, 3). However, there are also several other mechanisms of NF-κB activation known that have been shown to contribute to detrimental processes such as hypoxia/reoxygenation stress and to diseases such as muscular dystrophy that involves a calcium-dependent protease, calpain 3 (4-11). We have previously described yet another NF-κB regulatory mechanism that is constitutively activated in certain murine B-cell lines that involves degradation of IκBα in a manner dependent on calcium and calmodulin and a process that is sensitive to inhibition by the anticancer agent perillyl alcohol, which among other effects has been shown to inhibit a specific L-type calcium channel (12, 13). Pharmacologic evidence suggested that several major intracellular proteolytic systems, including proteasomes, calpains, caspases, lysosomal proteases, and the giant/tricorn protease, the latter of which can complement proteasome deficiency (14), are not involved in this unusual IκBα degradation and NF-κB activation mechanism (13). Moreover, *cis*-element analysis has shown that IκBα degradation involves distinct amino acid structures and does not require the canonical phosphorylation event or polyubiquitination mediated by β-TrCP (13, 15, 16), thereby partly explaining the lack of proteasome requirement. Although the precise proteolytic system involved in this "atypical" pathway remains to be determined, to distinguish it from all other known mechanisms, we have referred it as the "proteasome inhibitor–resistant" (PIR) pathway because of its high resistance to more

than 10 different proteasome inhibitors analyzed, including bortezomib (16). In addition to certain murine B lymphoma cell lines (e.g., WEHI231), normal murine splenic B cells, the human breast cancer cell line MDA-MB-463, and the human multiple myeloma (MM) cell line RPMI8226 have also been found to harbor constitutive NF-κB activity that is maintained by the PIR mechanism (12, 13, 15, 16).

Bortezomib, which potently blocks chymotryptic activity within the 26S proteasome, showed a significant overall response rate as a single agent against refractory MM in phase I and II clinical trials (3, 17). Because proteasomes are involved in a wide variety of intracellular and intercellular events, the precise molecular pathway(s) of bortezomib that gives rise to favorable clinical outcomes is unclear; however, modulation of many important pathways, including NF-κB, within the malignant cells has been implicated (18-21). Because MM pathogenesis also involves the critical participation of bone marrow microenvironment components, such as bone marrow stromal cells (BMSC), endothelial cells, and osteoclasts (22), bortezomib effects on these nonmalignant cells have also been implicated in clinical efficacy (22, 23). Although initial overall response rates to bortezomib are promising, the vast majority of patients who respond develop resistance to the drug over time. The exact mechanisms of bortezomib sensitivity and resistance *in vivo* in MM patients remain incompletely understood.

Because constitutive NF-κB activity is observed by immunofluorescence in virtually all primary MM samples analyzed (24, 25) and is implicated in chemoresistance of MM cells, here we investigated (*a*) the frequency of constitutive PIR NF-κB activity in a cohort of primary MM patient samples and (*b*) whether PIR NF-κB activation in MM cells is modulated by the presence of BMSCs derived from MM patients. Below, we describe a surprising finding that a constitutive NF-κB activity present in primary MM cells is frequently refractory to inhibition by bortezomib and that MM patient-derived BMSCs have the capacity to further increase this activity. This increase in constitutive NF-κB activity due to BMSCs is also seen in RPMI8226 cells, which correlated with increased bortezomib resistance *in vitro*. Our data provide the first insight into the potentially significant involvement of the PIR pathway of NF-κB activation in MM pathogenesis and resistance development.

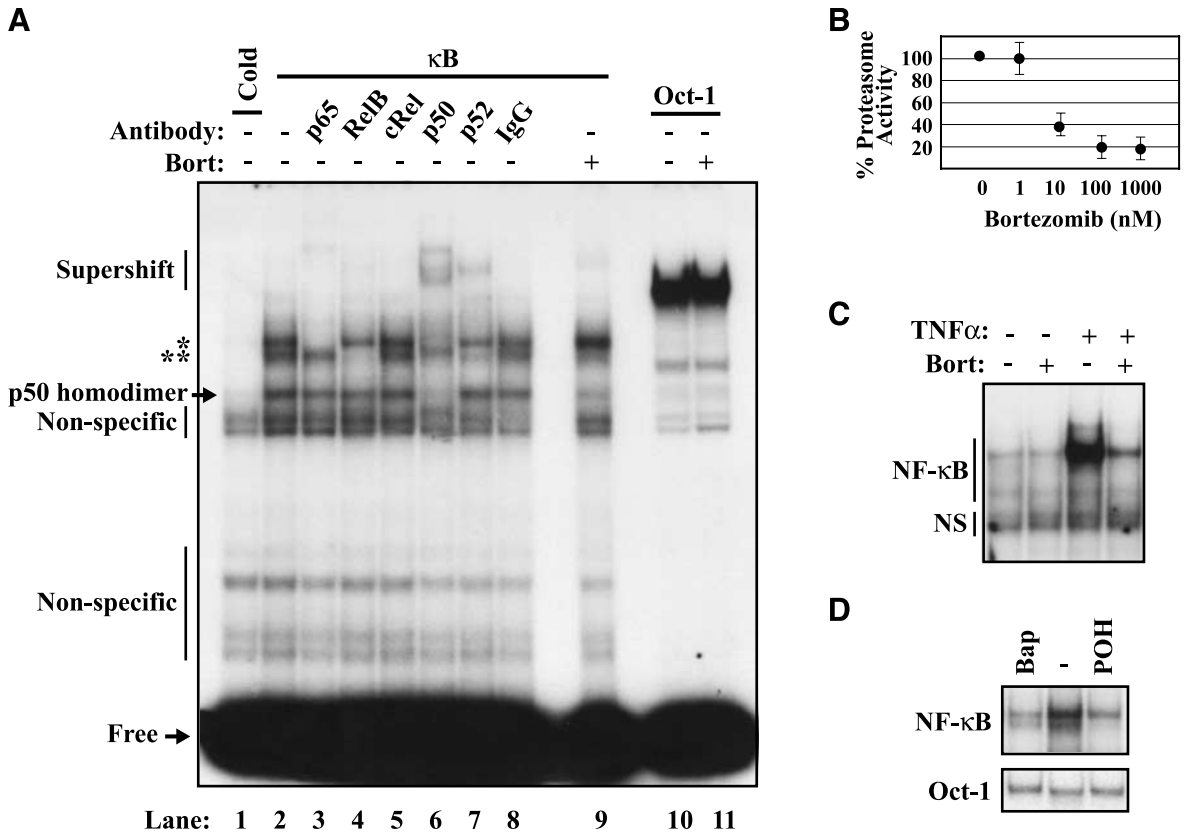

FIGURE 1. Constitutive NF-κB activity in the RPMI8226 cells is resistant to near-complete proteasome inhibition by bortezomib. **A.** Representative EMSA analysis of RPMI8226 cell extract using a ^{32}P-labeled Igκ-κB (*κB*) probe with or without cold probe competition (*Cold*) or using Oct-1 DNA probes. Where indicated, the DNA-binding assay was done in the presence of antibodies (*Antibody*) against the five NF-κB family members or a nonspecific IgG antibody control. RPMI8226 cells were treated with 4 h of 100 nmol/L bortezomib (*Bort*) and analyzed by EMSA where indicated. Probe not bound by protein in the DNA-binding assay migrates at the bottom of the gel (*Free*). Supershift analysis (*Supershift*) indicates that constitutive NF-κB activity in RPMI8226 cells is composed of two main complexes of interest: a p65:p50 dimer (*) and a RelB:p52 dimer (**). Nonspecific binding is also indicated. **B.** Analysis of percent proteasome inhibition by increasing doses of bortezomib in RPMI8226 using Proteo-Glo (Bio-Rad Laboratories) assay. Basal proteasomal activity for each cell type is assigned as 100% activity. **C.** EMSA of extracts isolated from RPMI8226 cells exposed to 100 nmol/L bortezomib for 4 h or 20 ng/mL TNFα for 30 min where indicated. **D.** EMSA of extracts isolated from RPMI8226 cells treated with 4 h of 1.0 mmol/L perillyl alcohol (*POH*) or 30 μmol/L BAPTA-AM (*Bap*).

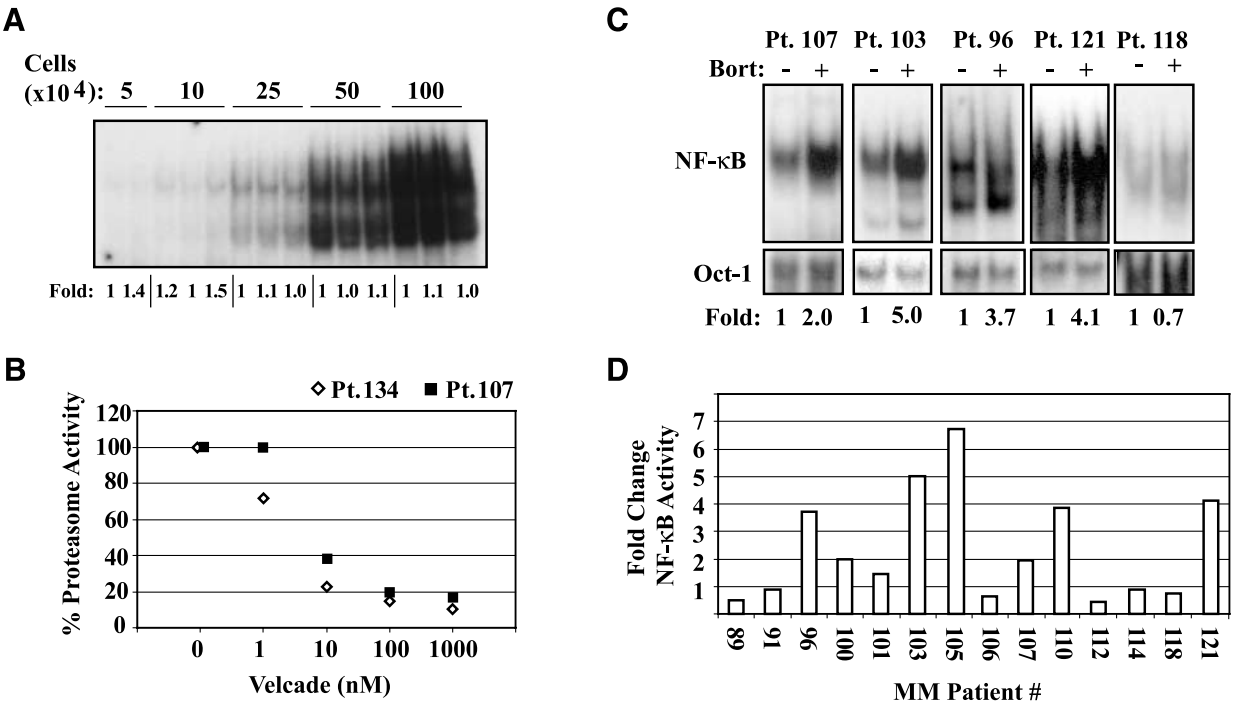

FIGURE 2. Primary MM cells display constitutive NF-κB activity that is largely resistant to high concentrations of bortezomib. **A.** Representative mini-EMSA, using whole-cell lysates from the indicated total cell numbers, fold induction as determined by phosphoimager is labeled below the gel. **B.** Analysis of percent proteasome inhibition by increasing doses of bortezomib in CD138$^+$ cells obtained from two MM patients using Proteo-Glo assay. Basal proteasomal activity for each cell type is assigned as 100% activity. **C.** EMSA analysis of lysates derived from CD138$^+$ cells isolated from the indicated patients and then treated with 100 nmol/L bortezomib for 4 h where indicated. Fold change in NF-κB activity corrected for Oct-1 DNA binding is displayed below the gels. **D.** Fold change NF-κB DNA binding, as measured by phosphoimage quantification corrected for Oct-1 DNA binding, induced by treatment with 4 h of 100 nmol/L bortezomib in CD138$^+$ cells from the indicated MM patients.

Results

Constitutive Bortezomib-Resistant NF-κB Activity Is Observed in Primary and Established Human MM Cells

Figure 1A shows electrophoretic mobility shift assay (EMSA) analysis of total cell extracts prepared from RPMI8226 cells along with supershift analysis using antibodies selective for NF-κB family members. Based on reactivity to these antibodies, the two major NF-κB complexes were assigned to be p50/p65 (RelA) and p52/RelB dimers (Fig. 1A, *lanes 3-8*). Increasing concentrations of bortezomib resulted in corresponding inhibition of the proteasomal activity in the RPMI8226 cells within 2 h (Fig. 1B); however, a high concentration could not block constitutive NF-κB activity (Fig. 1A). As a positive control to evaluate the efficacy of bortezomib, we tested its effect on tumor necrosis factor α (TNFα)-induced canonical activation and found, as expected, that 100 nmol/L bortezomib nearly completely blocked this activation (Fig. 1C). In contrast to bortezomib, treatment with a calcium chelator (BAPTA-AM) or perillyl alcohol, agents that selectively block the PIR activation pathway, effectively inhibited constitutive NF-κB activity (Fig. 1D).

Previous studies have shown that NF-κB is constitutively active in nearly all primary MM samples examined (24, 25). However, whether such activities are highly sensitive to bortezomib has not been reported. The existence of constitutive PIR NF-κB activity in RPMI8226 MM cells prompted us to test if constitutive NF-κB activity in a certain fraction of primary MM cells is also resistant to bortezomib. Because of the limited number of primary cells available, we developed a miniaturized EMSA ("mini-EMSA") that is reproducible with at least 50,000 cells per sample with a variance of ~10% (Fig. 2A). When we isolated CD138$^+$ MM cells from 14 patients, we found that all patients harbored some level of constitutive NF-κB activity. Treatment with 100 nmol/L bortezomib for 4 h induced near-complete proteasome inhibition in several primary MM cell samples tested (Fig. 2B); nevertheless, we were surprised to find that in many cases (10 of 14), this high-dose bortezomib failed to inhibit constitutive NF-κB activity, as measured by EMSA, in these primary cells (Fig. 2C). These experiments were done in duplicate when possible, but due to the limited number of available primary cells, we were unable to do triplicate experiments for statistical analysis. Paradoxically, in eight of these cases, NF-κB DNA binding was enhanced by treatment with bortezomib (Fig. 2C and D). Thus, these studies showed that bortezomib-resistant (or even bortezomib augmented) NF-κB activity is frequently detectable in primary MM samples.

Constitutive Bortezomib-Resistant NF-κB Activity Is Further Enhanced by BMSCs in Primary MM Cells

Although a considerable fraction of primary MM cell samples examined displayed bortezomib-resistant constitutive NF-κB activity, this observation was made in suspension culture conditions in the absence of bone marrow microenvironment

components. It was unclear how these primary MM cells would behave in the presence of patient-derived BMSCs. Thus, we established BMSC cultures from mononuclear cell preparations of MM patient bone marrow aspirates using the standard protocol (26). Next, we incubated primary MM cells on top of BMSCs and evaluated the consequent sensitivity of NF-κB activity to bortezomib in primary MM cells. Placing primary MM cells in coculture with MM-BMSCs caused further enhancement in NF-κB activity in most cases (Fig. 3, *lanes 2, 5, 8*, and *10*). Significantly, we were unable to block this BMSC-enhanced NF-κB activity using up to 100 nmol/L bortezomib in certain primary MM cells (Fig. 3, *lanes 3* and *11*). However, this was not a universal phenotype of MM cells because, in some cases, bortezomib was able to effectively inhibit BMSC-induced NF-κB activity in MM cells (Fig. 3, *lanes 6* and *9*). These data suggest that, depending on the MM samples, BMSC-induced NF-κB activity could be sensitive or insensitive to high-dose bortezomib treatment.

BMSCs Also Enhance PIR NF-κB Activation in RPMI8226 MM Cells

To gain insight into the significance of BMSC-induced NF-κB activation, we next turned to the more experimentally amenable RPMI8226 MM cell model. We placed RPMI8226 cells on top of BMSCs for 24 h as in the case with the primary MM cells and then did EMSA analysis using cell extracts obtained from the RPMI8226 cells. This analysis revealed enhanced NF-κB activity (up to 6-fold over basal activity; Fig. 3B). Oct-1 DNA binding was used as a loading control for all experiments (Fig. 3B, not shown in subsequent subpanels). Because removal of MM cells from BMSCs can be incomplete or possibly contaminated with BMSCs, we did a control experiment in which RPMI8226 cells and BMSCs either alone or in coculture for 24 h were collected either separately by mechanically tapping the plate to free RPMI8226 cells or by scraping all the cells together. We then did EMSA on RPMI8226 cells, BMSCs left behind, and those collected together. The NF-κB activity was observed in MM cell fractions and those collected together, but not in BMSC fractions (Fig. 3C). Thus, the bulk of the NF-κB activity comes from MM cells, which is not contaminated with that in BMSCs.

Time course analysis indicated that NF-κB DNA-binding activity was induced as early as 1 h but the peak activity was seen after 24 to 48 h of coculture (Fig. 3D). Interestingly, we observed variable degrees of increased NF-κB activity in

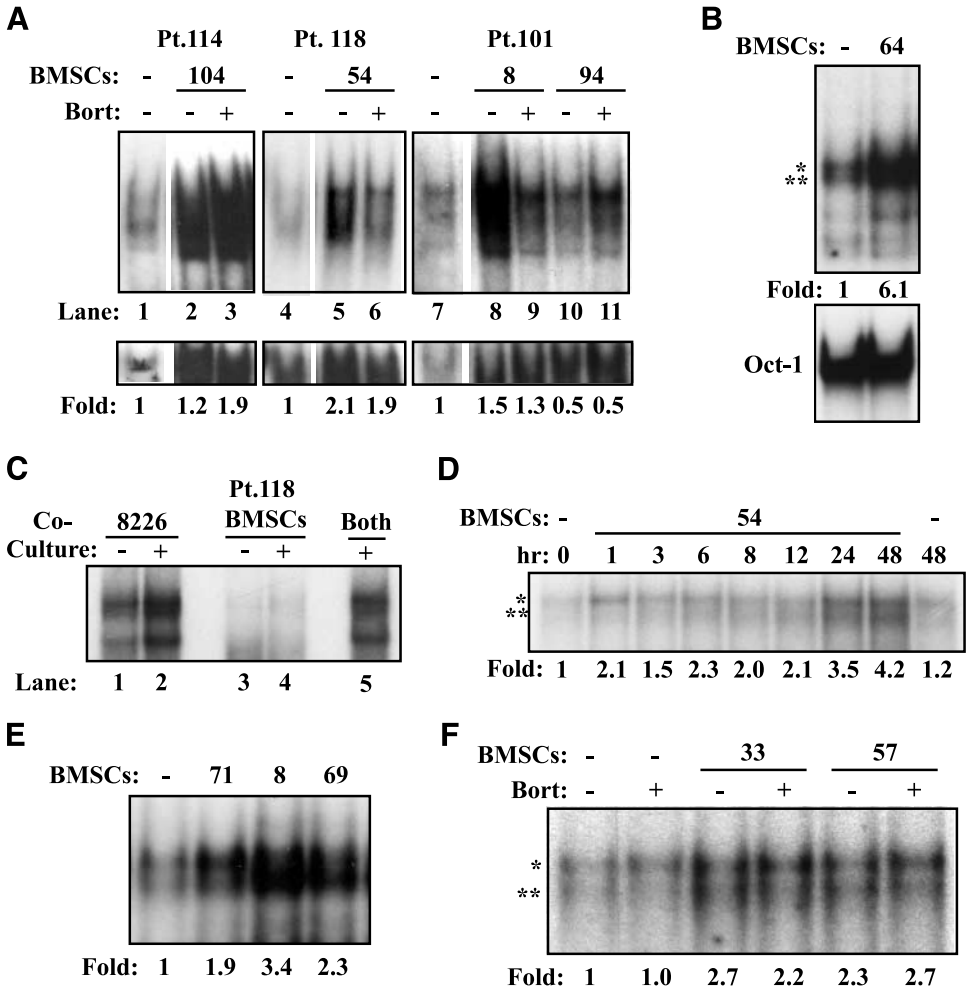

FIGURE 3. MM-BMSCs induce NF-κB activation in primary MM and RPMI8226 MM cells in a largely bortezomib-resistant manner. **A.** EMSA analysis of CD138$^+$ cells from the indicated MM patients cultured alone or with MM-BMSCs for 24 h. Bortezomib (100 nmol/L) was added 4 h before termination of coculture where indicated. Fold change in NF-κB activation is calculated and displayed as before. **B.** EMSA of RPMI8226 cells cultured alone or with Pt.64 BMSCs for 24 h. Oct-1 DNA binding was measured as a loading control. **C.** EMSA of RPMI8226 cells and MM-BMSCs culture alone (*lanes 1* and *3*), cultured together but separated for analysis (*lanes 2* and *4*), or cultured together and analyzed together (*lane 5*). **D.** EMSA of RPMI8226 cells cultured with MM-BMSCs for the indicated times. Fold change in NF-κB activity was measured as before and is displayed below the gel. **E.** EMSA of RPMI8226 cells cultured alone or with the indicated MM patients for 24 h. **F.** EMSA of RPMI8226 cells cultured alone or with the indicated MM patients for 24 h with 100 nmol/L bortezomib added for the last 4 h of coculture where indicated.

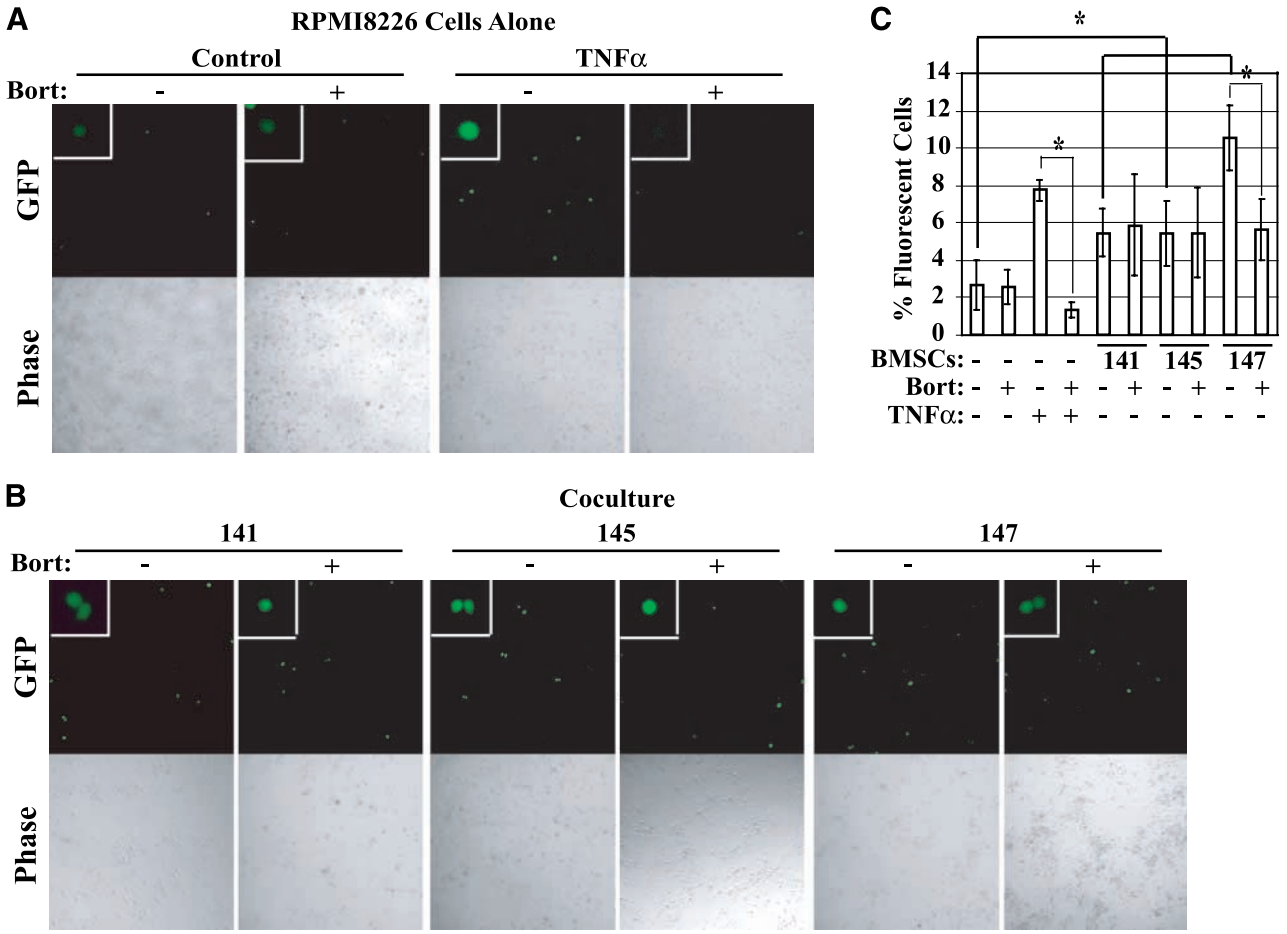

FIGURE 4. MM-BMSCs induce expression of nuclear NF-κB–dependent GFP reporter gene in RPMI8226 cells in a bortezomib-resistant manner. **A** and **B.** Fluorescent images (10×) of κB-GFP reporter-transfected RPMI8226 cells cultured alone (*RMPMI8226 Cells Alone*, **A**) or with BMSCs from the indicated patients (*Coculture*, **B**). Cells were treated with 1 ng/mL TNFα and/or 7.5 nmol/L bortezomib where indicated. Phase-contrast images of the same fields are shown below each fluorescent image. **C.** Percentage of green cells over total viable cells displayed on the *Y* axis for RPMI8226 cells alone or cocultured with BMSCs. Bars, SD. Statistical significance of the change in κB-reporter expression was determined by Mann-Whitney test with a 95% confidence interval.

RPMI8226 cells when they were cocultured with BMSCs derived from different MM patients (Fig. 3E). This indicated that different patient-derived BMSCs have differential NF-κB–inducing activity. Importantly, 100 nmol/L bortezomib failed to appreciably inhibit BMSC-enhanced NF-κB activity (Fig. 3F). Two other human MM cell lines, U266 and H929, also displayed inducible NF-κB activation when cocultured with MM-BMSCs, but the Jurkat human T-cell leukemia line did not respond to MM-BMSCs with respect to NF-κB activation (data not shown), suggesting the possibility of cell type selectivity of BMSC-inducible NF-κB activation.

To determine if the observed increases in NF-κB DNA-binding activity in RPMI8226 cells when cocultured with BMSCs were functionally relevant, we transiently transfected a *κB-GFP* reporter gene into RPMI8226 cells, cocultured them with BMSCs, and evaluated NF-κB–dependent green fluorescent protein (GFP) expression (Fig. 4). GFP expression was significantly increased by the presence of BMSCs derived from MM patients ($P = 0.01$; Fig. 4B). To evaluate if this NF-κB–dependent reporter gene induction is sensitive to inhibition by bortezomib, we next established the dose of bortezomib required to abrogate TNFα-induced activation. Incubation of MM cells with 7.5 nmol/L bortezomib was sufficient to nearly completely block activation (Fig. 4A). This concentration of bortezomib failed to significantly inhibit NF-κB–driven GFP expression in RPMI8226 cells grown on top of BMSCs ($P = 0.33$), with the exception of Pt.147 BMSCs where transcriptional activity was blocked by ~50% (Fig. 4B). This patient BMSCs also induced NF-κB activation as measured by EMSA that was partially bortezomib sensitive (data not shown). These findings together showed that certain MM patient-derived BMSCs have the capacity to induce NF-κB activation in RPMI8226 cells as measured by both EMSA and a κB-driven reporter assay.

BMSC-Enhanced NF-κB Activity Correlates with Increased Bortezomib Resistance in RPMI8226 Cells

Because NF-κB activity can increase drug resistance in several human cancer cell lines, including MM cells (27), we evaluated the relationship between the extent of NF-κB

activation and that of bortezomib resistance induced by BMSCs. We exposed RPMI8226 cells to varying doses of bortezomib for 24 h in the presence or absence of five patient BMSCs with different NF-κB–inducing potentials and analyzed the extent of apoptosis by determining the fraction of cells that displayed nuclear apoptotic morphology (Fig. 5A). As a control for effective drug concentration, we measured remaining proteasome activity in RPMI8226 cells alone or in the context of BMSCs to show that increasing concentrations of bortezomib inhibit the proteasome to a similar degree in both situations (Supplementary Fig. S1A). Our results show that BMSC-enhanced NF-κB activity strongly correlated with increased resistance of RPMI8226 to bortezomib-induced apoptosis (Fig. 5B). Simple linear regression analysis of the % protection of apoptosis conferred by each patient versus the fold NF-κB activity induced by each patient BMSC reveals a statistically significant correlation ($P = 0.001$). Thus, we conclude that BMSCs obtained from MM patients induced bortezomib resistance in RPMI8226 cells in part by inducing bortezomib-resistant NF-κB activation.

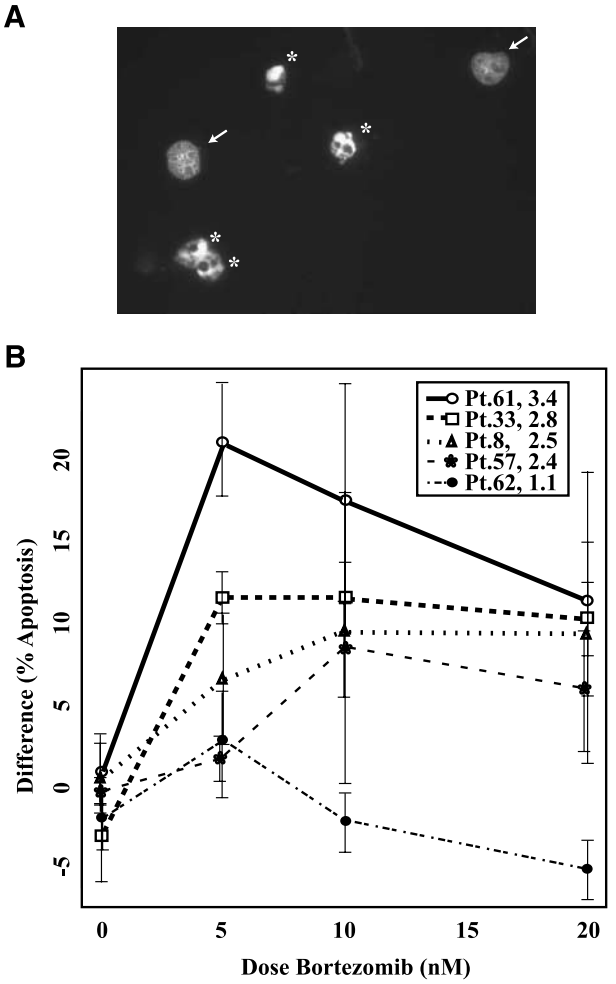

FIGURE 5. The degree of BMSC-induced NF-κB activity correlates with that of BMSC-induced protection of RPMI8226 MM cells against bortezomib-induced apoptosis. **A.** Representative 40× fluorescent micrograph of slides created in apoptosis assays quantified in **B.** Cells are stained with Hoechst 33342 and visualized through a 4′,6-diamidino-2-phenylindole filter. *Arrows,* representative cells that were considered nonapoptotic; *stars,* representative cells that were considered apoptotic. **B.** The difference between % apoptosis induced in RPMI8226 cells alone and that induced in RPMI8226 cells cocultured with BMSCs [*y* = % apoptosis (RPMI8226 alone) − % apoptosis (RPMI8226 + BMSC)] from the indicated patients is plotted on the *Y* axis versus increasing doses of bortezomib. The figure legend represents the patient numbers as well as fold change in NF-κB activity induced by each BMSC. Analysis of the correlation between % apoptosis difference (*Y axis*) and the fold change in NF-κB activity for each patient was done using linear regression fit model, which is detailed in Materials and Methods and displayed in Supplementary Fig. S1B.

Discussion

Many different molecular mechanisms of NF-κB activation have been described thus far, with the canonical and noncanonical pathways being the most widely studied (1). Indeed, in the context of MM, two recent reports found that ~20% of MM patients harbor one or more genetic aberrations in components of the NF-κB pathway, leading to constitutive canonical and/or noncanonical NF-κB activation (28, 29). Both groups began their studies with an unbiased, genetic screening approach to identify genetic aberrations in MM, and both uncovered targets primarily within the NF-κB signaling pathway. These seminal studies thus solidly implicated the NF-κB signaling system as one of the major targets of deregulation in MM pathogenesis.

The proteasome inhibitor bortezomib shows overall response rates in MM ranging from ~30% as a single agent to ~70% in combination with other targeted and traditional therapies (30). Given the extensive role of proteasomes in regulating intracellular processes, it is not surprising that the precise mechanism (or mechanisms) that mediates clinical efficacy of bortezomib in MM is not clearly defined. Previous metabolic labeling studies have shown that the vast majority of intracellular proteins are degraded by proteasomes (31), including many that regulate the activity of important transcription factors, including p53/MDM2, c-Jun NH_2-terminal kinase, hypoxia-inducible factor 1, c-Myc, and Notch (32-35). These pathways along with NF-κB have been implicated in mediating bortezomib effects on malignant cells (20, 36).

Unique among the various NF-κB activation mechanisms, the PIR pathway is highly resistant to bortezomib and other proteasome inhibitors (13, 15). If MM cells harbor constitutive NF-κB activity maintained by the PIR pathway, it is possible that this could contribute to the observed initial and/or developed clinical resistance to bortezomib. To gain initial insight into this possibility, we examined the presence of constitutive NF-κB activity in primary MM samples. We were surprised to find that a significant fraction of the samples analyzed showed the lack of inhibition of constitutive NF-κB activity by bortezomib, although bortezomib (*a*) nearly completely blocked proteasome activity in patient samples and (*b*) NF-κB activation by a canonical inducer, TNFα. Thus, we favor the notion that the lack of constitutive NF-κB inhibition in primary MM cells by bortezomib is not due to ineffective inhibition of proteasome activity in MM cells but rather this NF-κB activity is maintained by a mechanism that is independent of proteasomes. Alternatively, in the presence of a potent proteasome inhibitor, a bypass pathway may be invoked

to overcome the inhibition of proteasome activity. The PIR mechanism might represent one such bypass mechanism in MM cells. Moreover, in multiple cases, we observed paradoxical increases in NF-κB activity after treatment with bortezomib. Although NF-κB proteins are degraded by proteasomes (37-39), our limited Western blot analyses did not reveal any increases in p50, p65, and RelB protein levels in several MM patient samples analyzed.[7] Thus, there could also be a possible compensatory increase in the PIR mechanism in the presence of high bortezomib, leading to increased NF-κB activation in some cases. Given that bortezomib-resistant NF-κB activation has also been documented in endometrial, colon, and other cancer cell lines and/or samples (40, 41), bortezomib-resistant (or even bortezomib inducible) NF-κB activation might be more prevalent than currently perceived.

Because the role of the bone marrow microenvironment in providing a setting for MM tumor cell growth and survival is well documented (23), we also evaluated the effect of the presence of MM patient-derived BMSCs on the regulation of NF-κB. Previous studies have shown that these cells secrete factors, such as interleukin-6, TNFα, stromal cell–derived factor-1, insulin-like growth factor-I, B-cell–activating factor of the TNF family, and a proliferation-inducing ligand, which can mediate the protective effect on MM cells (22). Indeed, some of these factors have been shown to cause NF-κB activation in MM cells (23). Similarly, MM cells also secrete factors that can induce NF-κB activity in BMSCs to in turn produce MM supporting factors (23). Immunomodulatory drugs, such as thalidomide and Revlimid, are believed to modulate these MM-stromal interactions to induce clinical efficacy (23). Bortezomib has also been shown to block these mutual interactions by blocking NF-κB activation in BMSCs by interfering primarily with canonical and noncanonical pathways of NF-κB activation. Our current results introduce yet another possibility that involves the PIR pathway. We found that BMSCs derived from MM patients were capable of activating NF-κB in MM cell lines and primary cells to variable degrees in a manner that was largely resistant to bortezomib. Our preliminary studies suggest that the critical mediator (or mediators) of this inducible PIR activity is soluble and likely a peptide based on the presence of the activity in the soluble fraction of BMSC conditioned medium following 100,000 × *g* ultracentrifugation for 2 h, and its sensitivity to proteinase K and heat treatment. We have also tentatively eliminated the involvement of aforementioned factors by means of neutralizing antibodies. Further studies are thus required to elucidate the molecular mediator(s) of BMSC-induced PIR NF-κB activity. Identification of such a factor may provide deeper insight into both the signaling mechanism and biological role of the PIR pathway in MM pathobiology and other PIR-involving systems in general. This extracellular factor(s) could also represent a novel and useful biomarker for MM as well as a novel drug target for the treatment of this universally fatal disease.

[7] S. Markovina and S. Miyamoto, unpublished observations.

Materials and Methods

Cell Lines, Antibodies, and Chemicals

RPMI8226, U266, Jurkat, and H929 cell lines (American Type Culture Collection) were cultured in 37°C incubators with 5% CO_2 using DMEM (RPMI8226; Mediatech, Inc.) supplemented with 10% fetal bovine serum, 1,250 units of penicillin G (Sigma-Aldrich, Inc.), 0.5 mg of streptomycin sulfate (Sigma-Aldrich), and other supplements as per the American Type Culture Collection recommendations. DMEM with 20% fetal bovine serum and 1% L-glutamine ("BMSC medium") was used in coculture assays. p65 (C20) and RelB (C19) antibodies were purchased from Santa Cruz Biotechnology, p50 and p52 antibodies were purchased from Upstate Biotechnology, and the cRel antibody was obtained from Biomol. Bortezomib was commercially obtained from Millennium Pharmaceuticals, Inc. for experimental purposes. Human recombinant TNFα was purchased from Calbiochem. Perillyl alcohol was obtained from Sigma-Aldrich. BAPTA-AM was purchased from Merck.

Primary BMSCs

Primary human BMSCs were derived from deidentified fresh whole bone marrow aspirates. The aspirates were collected under the University of Wisconsin Institutional Review Board exemption protocol M-2004-1315 and thus were accompanied only by the patients' diagnosis of active myeloma (>10% plasma cells on Wright Giemsa–stained aspirate smears; analysis provided by Dr. C.P. Leith and other University of Wisconsin staff pathologists). Disease stage, treatment history and/or response, and other identifying patient characteristics are not available for the samples analyzed in this study. Mononuclear cells were isolated from aspirates as detailed in the Miltenyi Biotec MidiMACS bone marrow mononuclear cell protocol. Briefly, whole bone marrow is diluted with Iscove's modified Dulbecco's medium supplemented with heparin sulfate and DNase I and centrifuged with lymphocyte separation medium (Cellgro) to isolate the mononuclear population. Mononuclear cells were plated in BMSC medium and cultured at 37°C/5% CO_2. After 2 wk, nonadherent cells were washed off and one-half volume medium exchange was done every 3 d until a confluent layer of adherent stromal cells had formed. These cells were expanded and cryopreserved in liquid nitrogen. Repeated analysis of cryopreserved BMSCs from 22 patients, the NF-κB–inducing activity on RPMI8226 cells remained relatively constant over seven passages.

Primary MM Cells

To obtain primary MM cells, mononuclear cells isolated from patient bone marrow aspirates as described above were positively sorted using anti-CD138 magnetic microbeads and the MidiMACS cell sorting system following the manufacturer's protocol (Miltenyi Biotec) to >95% purity as determined by anti-CD138-PE staining and fluorescence-activated cell sorting analysis and cultured in 37°C/5% CO_2 incubators in BMSC medium.

Coculture Assays

BMSCs (6×10^4 per well) were plated in six-well dishes and allowed to form an adherent monolayer over 24 h. Media

were aspirated, and 10^6 RPMI8226 cells or 5×10^5 primary MM cells were plated over the monolayer. Where appropriate, 100 nmol/L bortezomib was added for the last 4 h of coculture. After 24 h, MM cells were mechanically detached from stromal cells, leaving ~5% of MM cells behind, mostly along the perimeter of the dish [as determined by immunofluorescence staining with anti-CD138 antibody (Miltenyi Biotec)]. The BMSC monolayer was undisturbed. For apoptosis assays, after 24 h of coculture, cells were treated with various doses of bortezomib for an additional 24 h before MM cells were removed for analysis.

Proteasome Activity Assay

Chymotryptic proteasomal activity was measured using the Proteasome-Glo Assay (Promega Corp.). Cells (10,000 per well) were plated in a black-walled 96-well tissue culture dish, allowed to rest for 3 h, and treated with increasing doses of bortezomib for 105 min before addition of the luminescent reagent as directed by the manufacturer. Luminescence was read on a Victor^{3}V 1420 Multilabel Counter from Perkin-Elmer. Relative light units for the no drug control were designated 100% proteasome activity, and the ratio of relative light units for each dose of bortezomib over control was used to determine the percentage decrease in chymotryptic activity.

DNA-Binding Analysis

EMSAs for cell lines were done as described previously (16). For primary MM cells, mini-EMSA was done by using the Mini-Protean 3 system (Bio-Rad Laboratories), 1-mm-thick gel, and 15-well comb to accommodate small amounts of protein obtained from primary MM cells. Briefly, CD138$^+$ cells were washed in 1× PBS and centrifuged in 200 μL PCR tubes at 5,000 rpm for 3 min at room temperature, and pellets were frozen at −70°C for later analysis. Frozen cell pellets were thawed on ice, lysed in Totex buffer with protease inhibitors (16) at 2.0×10^4 cells/μL, incubated on ice for 30 min with occasional tapping, and spun at 13,000 rpm for 10 min at 4°C. The resultant extracts in the supernatants were used for mini-EMSAs. Extract (1.5 μL) was incubated with 5× binding buffer, 0.1 mmol/L DTT, and 0.5 μL of radioactive probe on ice for 20 min as described in ref. 16. ^{32}P-labeled probe was added and samples were incubated at room temperature for 20 min. For each sample, one reaction with Igκ-κB probe and one with Oct-1 probe were run using Oct-1–binding levels as a loading control. Gels were run at 120 V for ~45 min, dried onto Whatman filters under vacuum, exposed to phosphoimage screen, and quantified using ImageQuant software. The volume of intensity using local area average background correction was calculated for cumulative NF-κB bands and the Oct-1 band.

GFP Reporter Assay

RPMI8226 cells (5×10^6) were transiently transfected using nucleofection (Amaxa, Inc.) with 3 μg of the 3×-κB-GFP reporter construct as described previously (42) with solution T, program G15. After a 24-h rest period, cells were split equally into culture alone or on top of 3×10^4 BMSC cells/mL plated 24 h previously and treated with 7.5 nmol/L bortezomib and/or 1 ng/mL TNFα where indicated. GFP expression was visualized 24 h later. Three random 10× fields of view were recorded through a GFP filter on a Zeiss Axiovert 200 M microscope using Axiovision 3.1 software and a Zeiss Axiocam to produce images. A 486-ms exposure time was used for each condition. The contrast of each of the images was adjusted to the exact same value using Adobe Photoshop (Adobe Systems, Inc.) to visualize GFP expression above untreated control levels. The remaining fluorescent cells were counted and displayed as a percentage of the total live cells counted in phase-contrast images of the same field. Representative 10× images were colored and adjusted with identical Photoshop methods for each, eliminating Photoshop bias.

Apoptosis Assay

Following culture and treatment as described in the Coculture Assays section, MM cells were cytospun onto microscope slides, fixed with 4% paraformaldehyde, and stained with Hoechst 33342 to label DNA. Slides were visualized through a 4′,6-diamidino-2-phenylindole filter. Cells (1,800) were counted for each condition (3×200 for each of three slides), and the percentage of apoptotic nuclei among them was quantified. Examples of what was considered normal versus apoptotic nuclei are presented.

Statistical Analysis

Fold induction of NF-κB activity was determined by phosphoimage quantification of enhanced NF-κB activity over constitutive activity, which was assigned an arbitrary value of 1. The change in NF-κB–dependent GFP expression induced by BMSC coculture was tested for significance using a two-sided Mann-Whitney test with a 95% confidence interval. Significant changes in GFP expression with and without bortezomib were determined by the Student's t test using a 95% confidence interval. The difference in bortezomib-induced apoptosis between RPMI8226 cells alone and coculture with different patient BMSCs is plotted as a function of bortezomib dose. A simple linear regression model was applied to analyze the correlation between % difference apoptosis and fold NF-κB activation, which is defined by the following equation: (apoptosis difference) = −8.2 + 5.8*(fold NF-κB activation), where the slope coefficient was significant ($P = 0.001$).

Disclosure of Potential Conflicts of Interest

The authors declare no potential conflicts of interest for this work.

Acknowledgments

We thank the Miyamoto lab members for helpful discussion, Dr. Alice Garry-McCoy for expert opinion and help with initiation of the project, and the Department of Hematology clinical trials staff for help with Institutional Review Board protocols and sample acquisition.

References

1. Perkins ND. Integrating cell-signalling pathways with NF-κB and IKK function. Nat Rev Mol Cell Biol 2007;8:49–62.

2. Adams J. The development of proteasome inhibitors as anticancer drugs. Cancer Cell 2004;5:417–21.

3. Richardson PG, Barlogie B, Berenson J, et al. A phase 2 study of bortezomib in relapsed, refractory myeloma. N Engl J Med 2003;348:2609–17.

4. Baghdiguian S, Richard I, Martin M, et al. Pathophysiology of limb girdle muscular dystrophy type 2A: hypothesis and new insights into the IκBα/NF-κB survival pathway in skeletal muscle. J Mol Med 2001;79:254–61.

5. Cogswell PC, Kashatus DF, Keifer JA, et al. NF-κB and IκBα are found in the mitochondria. Evidence for regulation of mitochondrial gene expression by NF-κB. J Biol Chem 2003;278:2963–8.

6. Fan C, Li Q, Ross D, Engelhardt JF. Tyrosine phosphorylation of IκBα activates NFκB through a redox-regulated and c-Src-dependent mechanism following hypoxia/reoxygenation. J Biol Chem 2003;278:2072–80.

7. Kato T, Jr., Delhase M, Hoffmann A, Karin M. CK2 is a C-terminal IκB kinase responsible for NF-κB activation during the UV response. Mol Cell 2003; 12:829–39.

8. Lee FY, Kim DW, Karmin JA, et al. μ-Calpain regulates receptor activator of NF-κB ligand (RANKL)-supported osteoclastogenesis via NF-κB activation in RAW 264.7 cells. J Biol Chem 2005;280:29929–36.

9. Romieu-Mourez R, Landesman-Bollag E, Seldin DC, Sonenshein GE. Protein kinase CK2 promotes aberrant activation of nuclear factor-κB, transformed phenotype, and survival of breast cancer cells. Cancer Res 2002;62:6770–8.

10. Schaecher K, Goust JM, Banik NL. The effects of calpain inhibition on IκBα degradation after activation of PBMCs: identification of the calpain cleavage sites. Neurochem Res 2004;29:1443–51.

11. Shen J, Channavajhala P, Seldin DC, Sonenshein GE. Phosphorylation by the protein kinase CK2 promotes calpain-mediated degradation of IκBα. J Immunol 2001;167:4919–25.

12. Berchtold CM, Chen KS, Miyamoto S, Gould MN. Perillyl alcohol inhibits a calcium-dependent constitutive nuclear factor-κB pathway. Cancer Res 2005;65: 8558–66.

13. Shumway SD, Miyamoto S. A mechanistic insight into a proteasome-independent constitutive inhibitor κBα (IκBα) degradation and nuclear factor κB (NF-κB) activation pathway in WEHI-231 B-cells. Biochem J 2004;380: 173–80.

14. Yao T, Cohen RE. Giant proteases: beyond the proteasome. Curr Biol 1999;9: R551–3.

15. O'Connor S, Markovina S, Miyamoto S. Evidence for a phosphorylation-independent role for Ser 32 and 36 in proteasome inhibitor-resistant (PIR) IκBα degradation in B cells. Exp Cell Res 2005;307:15–25.

16. O'Connor S, Shumway SD, Amanna IJ, Hayes CE, Miyamoto S. Regulation of constitutive p50/c-Rel activity via proteasome inhibitor-resistant IκBα degradation in B cells. Mol Cell Biol 2004;24:4895–908.

17. Adams J, Palombella VJ, Sausville EA, et al. Proteasome inhibitors: a novel class of potent and effective antitumor agents. Cancer Res 1999;59:2615–22.

18. Hideshima T, Mitsiades C, Akiyama M, et al. Molecular mechanisms mediating antimyeloma activity of proteasome inhibitor PS-341. Blood 2003;101: 1530–4.

19. Mitsiades N, Mitsiades CS, Poulaki V, et al. Biologic sequelae of nuclear factor-κB blockade in multiple myeloma: therapeutic applications. Blood 2002; 99:4079–86.

20. Nencioni A, Grunebach F, Patrone F, Ballestrero A, Brossart P. Proteasome inhibitors: antitumor effects and beyond. Leukemia 2007;21:30–6.

21. Obeng EA, Carlson LM, Gutman DM, Harrington WJ Jr, Lee KP, Boise LH. Proteasome inhibitors induce a terminal unfolded protein response in multiple myeloma cells. Blood 2006;107:4907–16.

22. Anderson KC. Targeted therapy of multiple myeloma based upon tumor-microenvironmental interactions. Exp Hematol 2007;35:155–62.

23. Hideshima T, Mitsiades C, Tonon G, Richardson PG, Anderson KC. Understanding multiple myeloma pathogenesis in the bone marrow to identify new therapeutic targets. Nat Rev Cancer 2007;7:585–98.

24. Bharti AC, Shishodia S, Reuben JM, et al. Nuclear factor-κB and STAT3 are constitutively active in $CD138^+$ cells derived from multiple myeloma patients, and suppression of these transcription factors leads to apoptosis. Blood 2004;103: 3175–84.

25. Podar K, Hideshima T, Chauhan D, Anderson KC. Targeting signalling pathways for the treatment of multiple myeloma. Expert Opin Ther Targets 2005; 9:359–81.

26. Gregoretti MG, Gottardi D, Ghia P, et al. Characterization of bone marrow stromal cells from multiple myeloma. Leuk Res 1994;18:675–82.

27. Karin M. Nuclear factor-κB in cancer development and progression. Nature 2006;441:431–6.

28. Annunziata CM, Davis RE, Demchenko Y, et al. Frequent engagement of the classical and alternative NF-κB pathways by diverse genetic abnormalities in multiple myeloma. Cancer Cell 2007;12:115–30.

29. Keats JJ, Fonseca R, Chesi M, et al. Promiscuous mutations activate the noncanonical NF-κB pathway in multiple myeloma. Cancer Cell 2007;12: 131–44.

30. Merchionne F, Perosa F, Dammacco F. New therapies in multiple myeloma. Clin Exp Med 2007;7:83–97.

31. Rock KL, Gramm C, Rothstein L, et al. Inhibitors of the proteasome block the degradation of most cell proteins and the generation of peptides presented on MHC class I molecules. Cell 1994;78:761–71.

32. Ehebauer M, Hayward P, Martinez-Arias A. Notch signaling pathway. Sci STKE 2006;2006:cm7.

33. Hunter T, Karin M. The regulation of transcription by phosphorylation. Cell 1992;70:375–87.

34. Sears R, Leone G, DeGregori J, Nevins JR. Ras enhances Myc protein stability. Mol Cell 1999;3:169–79.

35. Wei W, Yu XD. Hypoxia-inducible factors: crosstalk between their protein stability and protein degradation. Cancer Lett 2007;257:145–56.

36. Richardson PG, Mitsiades C, Hideshima T, Anderson KC. Proteasome inhibition in the treatment of cancer. Cell Cycle 2005;4:290–6.

37. Lawrence T, Bebien M, Liu GY, Nizet V, Karin M. IKKα limits macrophage NF-κB activation and contributes to the resolution of inflammation. Nature 2005; 434:1138–43.

38. Ryo A, Suizu F, Yoshida Y, et al. Regulation of NF-κB signaling by Pin1-dependent prolyl isomerization and ubiquitin-mediated proteolysis of p65/RelA. Mol Cell 2003;12:1413–26.

39. Tanaka T, Grusby MJ, Kaisho T. PDLIM2-mediated termination of transcription factor NF-κB activation by intranuclear sequestration and degradation of the p65 subunit. Nat Immunol 2007;8:584–91.

40. Dolcet X, Llobet D, Encinas M, et al. Proteasome inhibitors induce death but activate NF-κB on endometrial carcinoma cell lines and primary culture explants. J Biol Chem 2006;281:22118–30.

41. Nagy K, Szekely-Szuts K, Izeradjene K, et al. Proteasome inhibitors sensitize colon carcinoma cells to TRAIL-induced apoptosis via enhanced release of Smac/DIABLO from the mitochondria. Pathol Oncol Res 2006;12:133–42.

42. Wuerzberger-Davis SM, Chang PY, Berchtold C, Miyamoto S. Enhanced G_2-M arrest by nuclear factor-κB-dependent p21waf1/cip1 induction. Mol Cancer Res 2005;3:345–53.

Molecular Cancer Research

Bortezomib-Resistant Nuclear Factor-κB Activity in Multiple Myeloma Cells

Stephanie Markovina, Natalie S. Callander, Shelby L. O'Connor, et al.

Mol Cancer Res 2008;6:1356-1364.